



CLASSICALLY FORBIDDEN ASKARYAN RADIATION

A DECADE OF EXPLORATION IN ANTARCTICA IN THE SEARCH FOR
COSMIC NEUTRINOS

Dr. Jordan Hanson

May 7, 2018

Whittier College

OUTLINE

OUTLINE

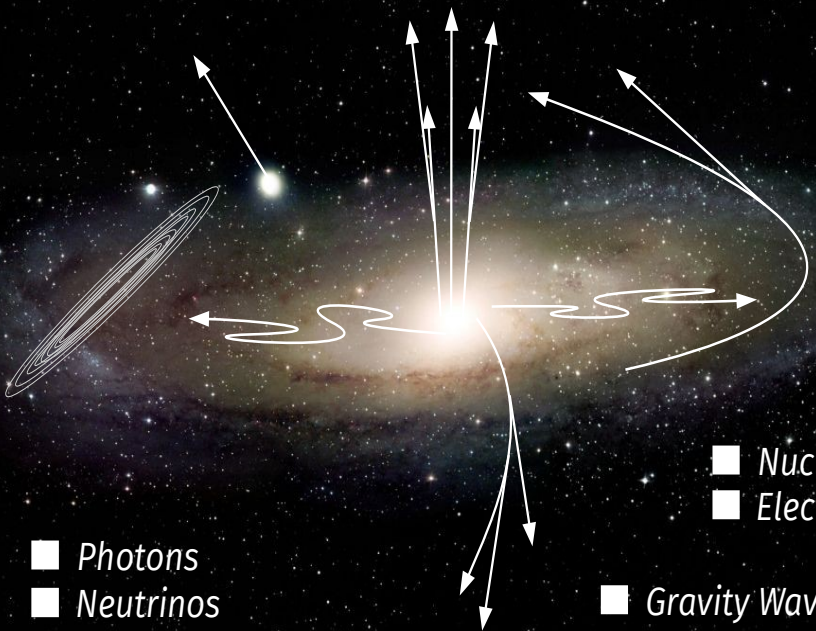
- I. Cosmic rays ... *Ultra-high energy particles from space*
- II. Askaryan radiation ... *Classical and quantum physics*
- III. Antarctica... *Field of Askaryan-based cosmic ray science*
- IV. Propagation in Antarctic ice ... *New results*

I. COSMIC RAYS ... *ULTRA-HIGH ENERGY* *PARTICLES FROM SPACE*

COSMIC RAYS ... DEFINITION OF A COSMIC RAY

Definition of a Cosmic Ray *A cosmic ray is a relativistic particle in deep space.* Often in science, decades of work can be encapsulated in a single statement. Cosmic rays, like all other particles, have the following properties:

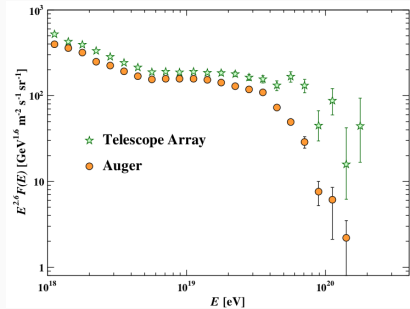
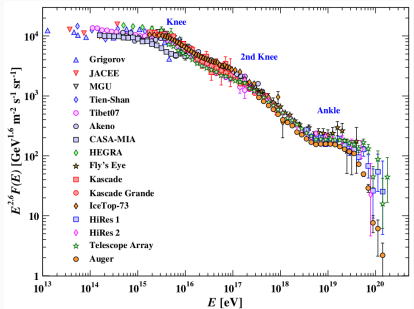
- Total Energy and Rest Mass
- N/Z , the number of nucleons, the number of protons
- Momentum, in a certain direction
- Flux, in units of particles per area per solid angle per time
- Particle type...



■ Photons
■ Neutrinos

■ Nuclei
■ Electrons
■ Gravity Waves

COSMIC RAYS



UHE flux spans *seven orders of magnitude* in energy per nucleus.

COSMIC RAYS

Domenico Pacini, electroscope discharge vs. depth underwater, Livorno, Italy, 1911. *Victor Hess, electroscope discharge vs. balloon height, Austria, 1911-12*

Robert Millikan and Arthur Compton. Research confirmed that particles were from space, and charged. 1930s Chicago, California

Charles Wilson wins *Nobel Prize* for invention of cloud chamber, 1927. Allows photography of sub-atomic tracks

Carl Anderson and Seth Neddermeyer (Caltech) discover muon and positron, Anderson shares 1936 *Nobel Prize* with Victor Hess.

Bruno Rossi (Chicago) discovers muon decay, Mt. Evans, 1939

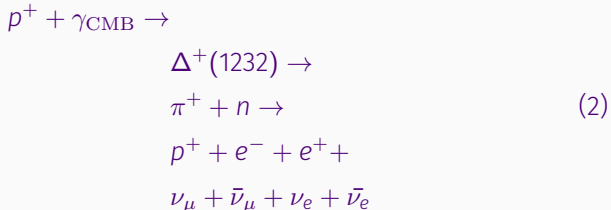
The Solar Neutrino Problem, neutrino oscillations, and cosmic neutrinos. John Bahcall, Ray Davis, Art McDonald and others, *two Nobel prizes in 2002 and 2015*

COSMIC RAYS

Finding the original trajectories would allow determination of the sources, but the original trajectories are lost during passage through electromagnetic fields. Further, the highest energy cosmic rays undergo *energy loss mechanisms* like Eq. 1.



Enter the GZK effect¹ (2008) [1]:



¹ $p^+ + \gamma_{\text{CMB}} \rightarrow \Delta^+(1232) \rightarrow \pi^0 + p^+ \rightarrow p^+ + \gamma\gamma$ is also a possibility.

COSMIC RAYS

Neutrinos offer a UHE messenger capable of revealing the UHE cosmic ray accelerators, and the chance to observe UHE electro-weak interactions on Earth². But how can we observe them?

²A typical UHE- ν interaction would be a factor of 100 higher in COM energy than the LHC.

II. ASKARYAN RADIATION ... CLASSICAL AND QUANTUM PHYSICS

ASKARYAN RADIATION

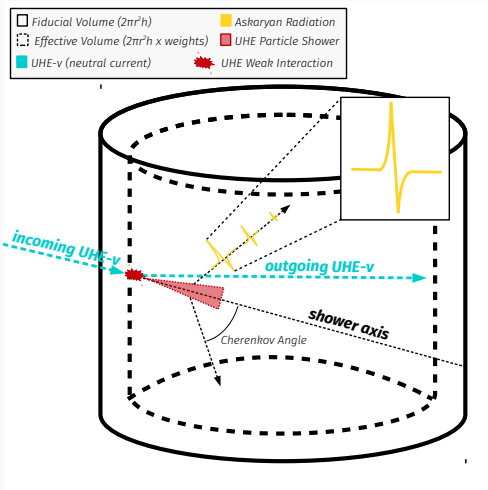


Figure 3: The concepts of *fiducial* and *effective* volume, $\text{UHE-}\nu$, **Askaryan radiation**, **UHE cascade**, and **attenuation length**.

ASKARYAN RADIATION

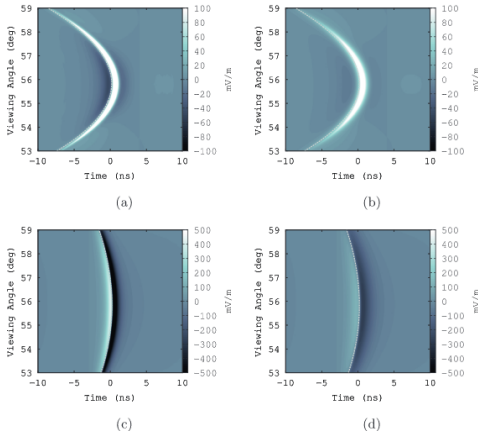


Fig. 3. Contours of $\delta_0 \cdot \mathbf{E}(\mathbf{r})$, for a cascade energy of 1000 PeV. (a) $R=1000$ m, lateral ICD width of 5 cm. (b) $R=1000$ m, lateral ICD width of 10 cm. (c) $R=200$ m, lateral ICD width of 5 cm. (d) $R=200$ m, lateral ICD width of 10 cm. The LPM effect has been taken into account. See text for details.

Figure 4: One vector component of Askaryan radiation [8].

ASKARYAN RADIATION

82

J.C. Hanson, A.L. Connolly / Astroparticle Physics 91 (2017) 75–89

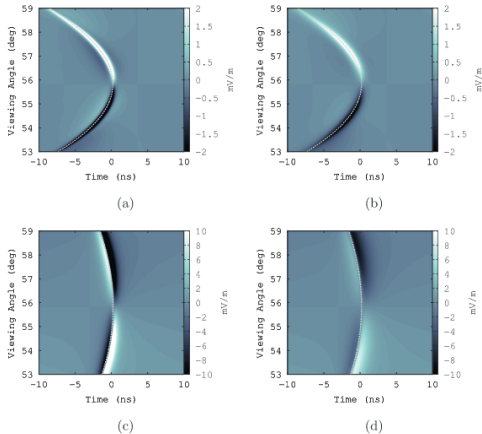


Fig. 4. Contours of $\delta_{\text{z}} \cdot \mathbf{E}(t)$, for a cascade energy of 1000 PeV. (a) $R=1000$ m, lateral ICD width of 5 cm, (b) $R=1000$ m, lateral ICD width of 10 cm, (c) $R=200$ m, lateral ICD width of 5 cm, (d) $R=200$ m, lateral ICD width of 10 cm. In all cases, the gray dashed line represents the causality requirement. See text for details.

Figure 5: The other vector component of Askaryan radiation [8].

ASKARYAN RADIATION

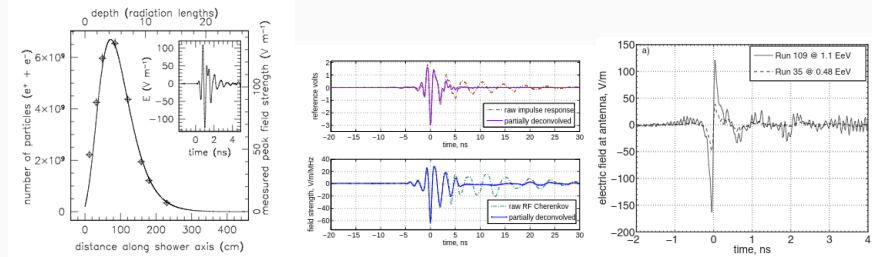


Figure 6: The Askaryan effect has been reported in beamline tests [6][11][12]. Electrons and gamma-rays were used to strike blocks of salt and ice to create radio-frequency (RF) pulses.

ASKARYAN RADIATION

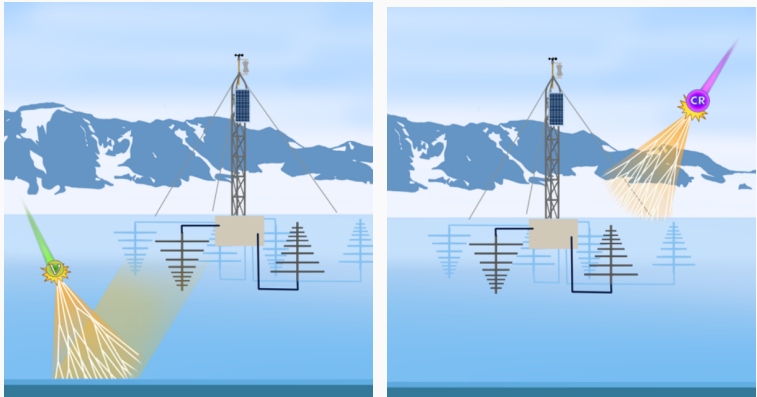


Figure 7: With ice as the target the RF pulses become detectable.

ASKARYAN RADIATION

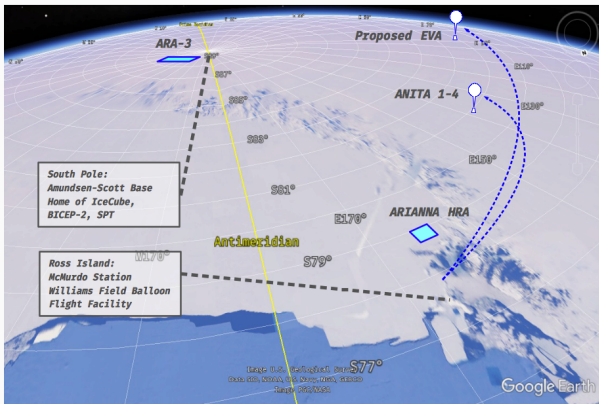


Figure 8: Antarctic ice serves as both target and landscape.

ASKARYAN RADIATION

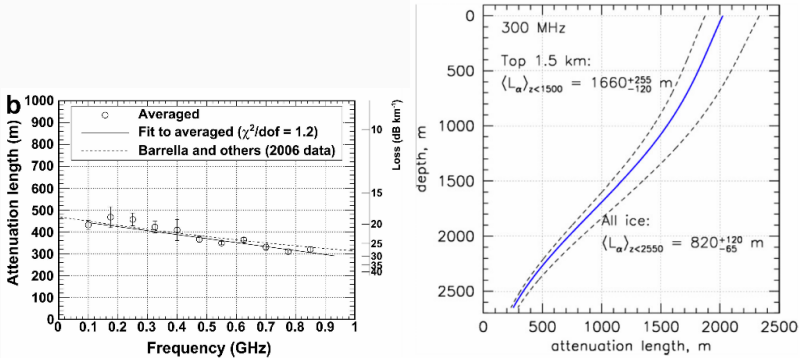


Figure 9: (Left) Attenuation length in Moore's Bay versus frequency, as measured from radio-echo sounding. (Right) Attenuation length near the South Pole, as modeled from 300 MHz measurement and temperature profile [2][7].

III. ANTARCTICA ... FIELD OF ASKARYAN-BASED COSMIC RAY SCIENCE

ANTARCTICA

Antarctic Ross Ice Shelf Antenna Neutrino Array - ARIANNA



Figure 10: Moore's Bay, with an ARIANNA station visible.

Antarctic Ross Ice Shelf Antenna Neutrino Array - ARIANNA

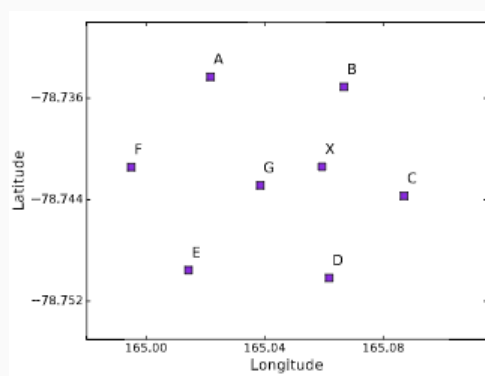


Figure 11: Layout of ARIANNA.

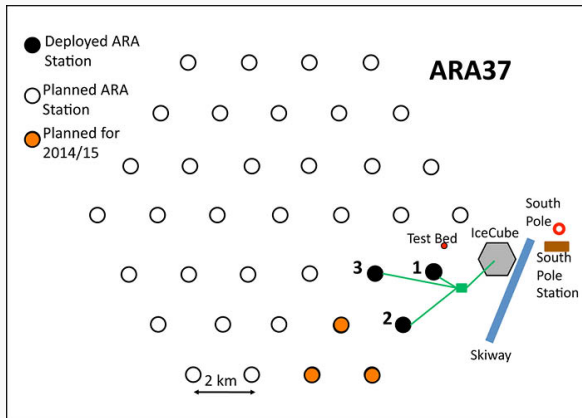
Askaryan Radio Array - ARA

Figure 12: Schematic of Askaryan Radio Array (more detectors online now).

Askaryan Radio Array - ARA

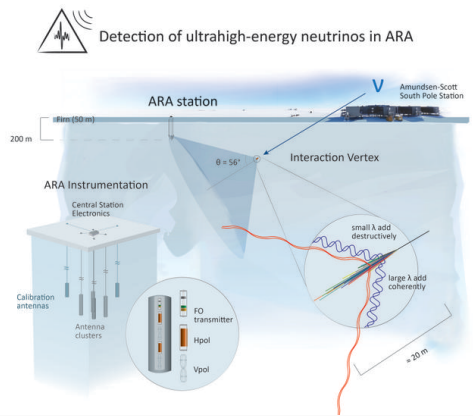


Figure 13: Schematic of Askaryan Radio Array (more detectors online now).

ANTARCTICA

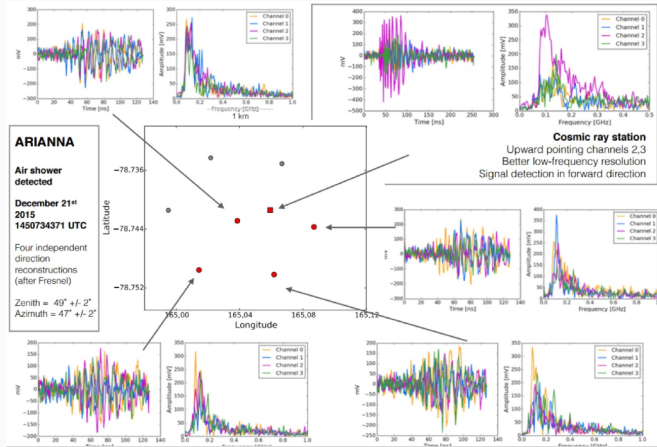


Figure 14: Summary of the ARIANNA detection of 1000 PeV cosmic-rays.

ANTARCTICA

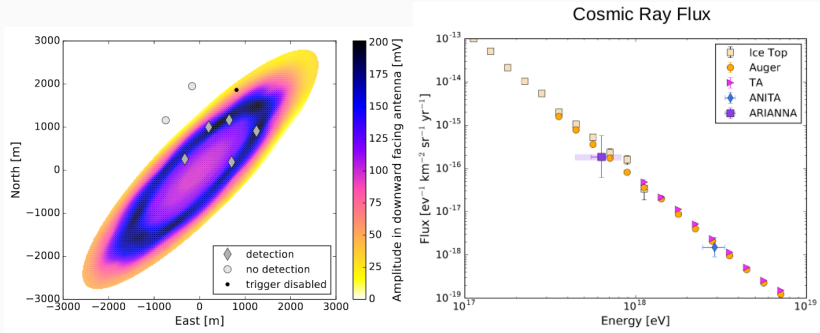


Figure 15: Summary of the ARIANNA detection of 1000 PeV cosmic-rays [5].

ANTARCTICA

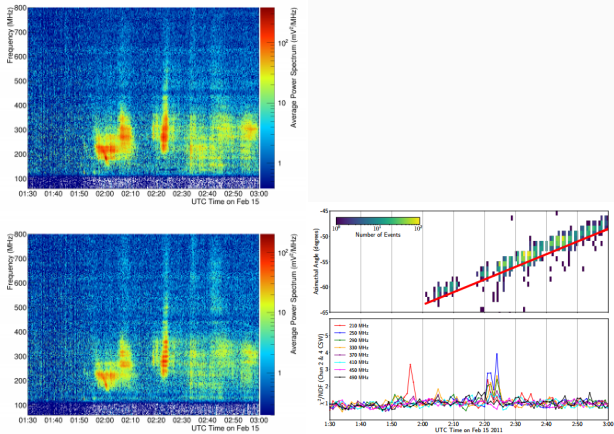


Figure 16: Observation of solar flare by Askaryan Radio Array (courtesy of B. Clarke, Ohio State, in press).

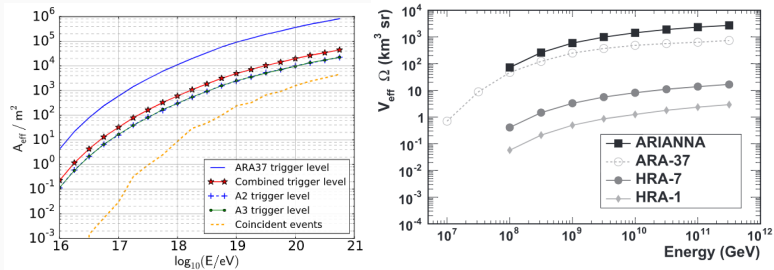


Figure 17: Effective area/volume of the ARIANNA and ARA experiments [3][4].

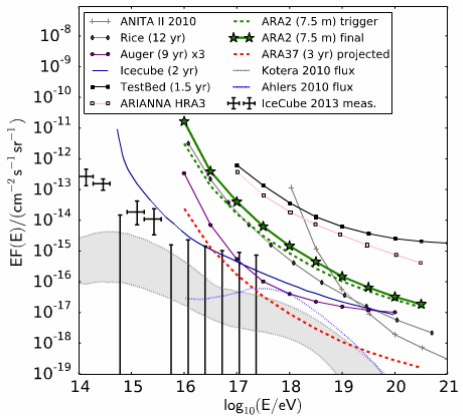


Figure 18: Flux limit summary figure [3].

Key to the field:

1. With steadily *increasing effective volume*, UHE- ν from GZK will be detected
 - 1.1 Time, resources
 - 1.2 Successful deployments
 - 1.3 Potential merger of ARIANNA and ARA
2. Sensitivity is based on *volumetric scaling*, and **classical** RF propagation.
3. The *effective volume* calculations would have to change dramatically if *non-classical* propagation were observed.

What do we mean by *classical* versus *non-classical*?

IV. PROPAGATION IN ANTARCTIC ICE ... *NEW RESULTS*

PROPAGATION IN ANTARCTIC ICE

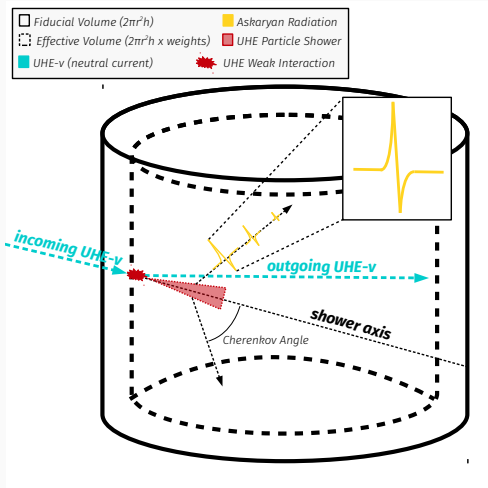


Figure 19: The Askaryan radiation must propagate through ice with changing density.

PROPAGATION IN ANTARCTIC ICE

Observation of classically ‘forbidden’ electromagnetic wave propagation and implications for neutrino detection.

S. W. Barwick^a, E. C. Berg^a, D. Z. Besson^{b,c}, G. Gaswint^a, C. Glaser^a, A. Hallgren^d, J. C. Hanson^e, S. R. Klein^f, S. Kleinfelder^g, L. Köpke^h, I. Kravchenkoⁱ, R. Lahmann^j, U. Latif^k, J. Nam^k, A. Nelles^a, C. Persichilli^a, P. Sandstrom^l, J. Tatar^{a,m}, E. Unger^d

^a Department of Physics & Astronomy 4129 Frederick Reines Hall, University of California, Irvine, CA 92697-4575

^b Dept. of Physics and Astronomy, Univ. of Kansas, Lawrence, KS 66045.

^c National Research Nuclear University, Moscow Engineering Physics Institute, 31 Kashirskoye Highway, Rossia 115409

^d Uppsala University Department of Physics and Astronomy, Regementsvgen 1, SE-752 37 Uppsala, Sweden

^e Whittier College Department of Physics, 13406 E. Philadelphia St., Whittier, CA 90602

^f Lawrence Berkeley National Laboratory, 1 Cyclotron Rd. Berkeley, CA, 94720

^g Department of Electrical Engineering and Computer Science, University of California, Irvine, CA 92697-4575

^h Institute of Physics, University of Mainz, Staudinger Weg 7, D-55099 Mainz, Germany

ⁱ Dept. of Physics and Astronomy, Univ. of Nebraska-Lincoln, NE, 68588

^j ECAP, Friedrich-Alexander Universität Erlangen-Nürnberg, Erwin-Rommel-Str. 1, 91058 Erlangen, Germany

^k Leung Center for Cosmology and Particle Astrophysics; National Taiwan University; No. 1, Sec. 4, Roosevelt Road Taipei, 10617, Taiwan (R.O.C)

^l Dept. of Physics and Wisconsin IceCube Particle Astrophysics Center, University of Wisconsin, Madison, WI 53706, USA

^m Research Cyberinfrastructure Center, University of California, Irvine, CA 92697

PROPAGATION IN ANTARCTIC ICE

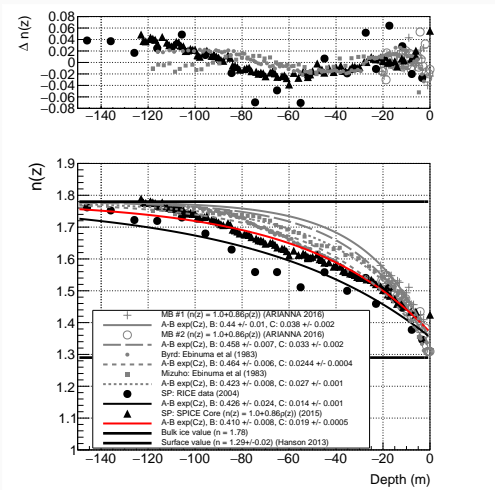


Figure 20: The density profile leads depth-dependence in $n(z)$.

PROPAGATION IN ANTARCTIC ICE

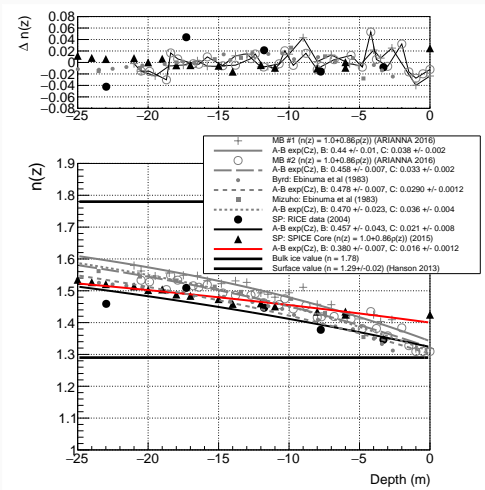


Figure 21: The density profile leads depth-dependence in $n(z)$.

PROPAGATION IN ANTARCTIC ICE

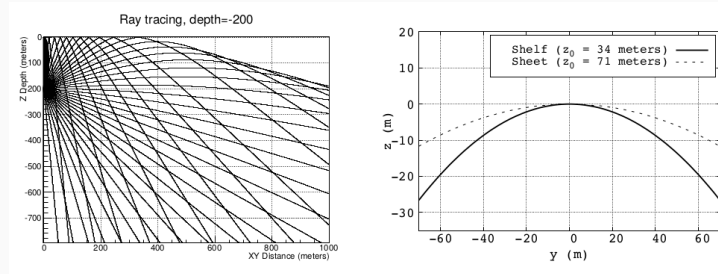


Figure 22: The goal of *ray-tracing* is to predict the path of the Askaryan pulse, given the initial trajectory and the $n(z)$ profile. The effective volumes of ARIANNA and ARA depend on the accuracy of ray-tracing algorithms. (Left) Output of AraSim ray-tracing algorithms. (Right) Near-surface expectation (see below).

PROPAGATION IN ANTARCTIC ICE

Those algorithms are false.

PROPAGATION IN ANTARCTIC ICE

The compressibility χ of a simple block of material with volume $l^2 \Delta z' = v$ and uniform pressure p is defined as

$$\chi = -\frac{1}{v} \frac{\Delta v}{\Delta p} \quad (3)$$

Rearranging,

$$-\frac{\Delta v}{v} = \chi \Delta p \quad (4)$$

Suppose that a block comprised of snow, ice and air, known as *firn*, with volume $l^2 \Delta z' = v$ is compressed by a pressure p originating from a force in the z -direction. The density of the uncompressed block is $m/(l^2 \Delta z')$, where m is the mass. The compressed length of the block becomes $\Delta z' - \epsilon = \Delta z$, the volume decreases by $\Delta v = v_f - v_i = -\epsilon l^2$.

PROPAGATION IN ANTARCTIC ICE

The change in density is

$$\Delta\rho = \rho_f - \rho_i = m \left(\frac{1}{v_f} - \frac{1}{v_i} \right) = -\frac{m\Delta v}{v_f v_i} = -\rho_f \frac{\Delta v}{v} \quad (5)$$

From now on, the initial volume is $v_i = v$. Substituting Eq. 4 into Eq. 5,

$$\Delta\rho = \rho_f \chi \Delta p \quad (6)$$

$$\Delta p = (\chi \rho_f)^{-1} \Delta\rho \quad (7)$$

Dividing both sides by Δz , taking the limit $\Delta z \rightarrow 0$, and relabelling ρ_f to simply ρ :

PROPAGATION IN ANTARCTIC ICE

$$\frac{\Delta p}{\Delta z} = (\rho_f \chi)^{-1} \frac{\Delta \rho}{\Delta z} \quad (8)$$

$$p' = (\chi \rho)^{-1} \rho' \quad (9)$$

From here, we can make one of three assumptions:

1. $(\chi_0 \rho_0)^{-1}$ is an empirical constant
 2. $\chi(z)$ depends on depth, and $\rho = \rho_0$ is some empirical constant
 3. $(\chi(z) \rho(z))^{-1}$ depends on depth
-

PROPAGATION IN ANTARCTIC ICE

Let the region of firn be described by N firn blocks labelled by j , with varying density ρ_j . Let the snow surface correspond to $j = N, z = 0$, and the beginning of solid ice (the bottom of the firn) correspond to $j = 0, z = -h$. Each compressed block has a height Δz , and a volume $v = l^2 \Delta z$. The normal force $f = p_j A$ on block j must oppose the weight of block j , and the total mass M of the firn above block j :

$$l^2 p_j = g (m_j + M) \quad (10)$$

$$M = \sum_{i=j+1}^N m_i = \sum_{i=j+1}^N \rho_i l^2 \Delta z \quad (11)$$

$$m_j = \rho_j l^2 \Delta z \quad (12)$$

PROPAGATION IN ANTARCTIC ICE

Combining Eqs. 10-12, and cancelling the common l^2 factor,

$$p_j = g \sum_{i=j}^N \rho_i \Delta z \quad (13)$$

Take the limit $\Delta z \rightarrow 0$:

$$p(z) = g \int_z^0 \rho(z') dz' \quad (14)$$

Reversing the limits of integration, and taking the derivative of both sides:

$$p'(z) = -g(\rho(z) - \rho(0)) \quad (15)$$

PROPAGATION IN ANTARCTIC ICE

Substituting Eq. 9 into Eq. 15, assuming $(\chi_0 \rho_0)^{-1}$ is some coefficient,

$$\rho' = - (g \chi_0 \rho_0) (\rho(z) - \rho(0)) \quad (16)$$

Differentiating once more yields:

$$\rho'' = - (g \chi_0 \rho_0) \rho' \quad (17)$$

Notice that, from the units, $z_0^{-1} = (g \chi_0 \rho_0)$.

$$\rho'' = -z_0^{-1} \rho' \quad (18)$$

Up to this point, we have been measuring z downwards, so we adopt $z \rightarrow -z$ to measure depth in the usual way:

$$\rho'' = z_0^{-1} \rho' \quad (19)$$

PROPAGATION IN ANTARCTIC ICE

There are two boundary conditions for the second-order differential equation: the surface behavior $\rho(0) = \rho_s$, and the deep behavior $\lim_{z \rightarrow -\infty} \rho(z) = \rho_i$. Letting $\Delta\rho = \rho_i - \rho_s$, the following equation is a solution to Eq. 17:

$$\boxed{\rho(z) = \rho_i - \Delta\rho \exp(z/z_0)} \quad (20)$$

Although the depth-scale z_0 of the firn is controlled by the compressibility of the firn ice χ_0 , this relation is empirical until the compressibility depth-dependence is specified. For ice and snow: $n(z) = 1 + b\rho$. Thus,

$$\boxed{n(z) = n_{ice} - \Delta n e^{z/z_0}} \quad (21)$$

PROPAGATION IN ANTARCTIC ICE

What are the measured values of z_0 ?

Ref./Location	Δn	n_s	z_0 (m)
MB#1/Moore's Bay	0.46 ± 0.01	1.32 ± 0.01	34.5 ± 2
MB#2/Moore's Bay	0.481 ± 0.007	1.299 ± 0.007	37 ± 1
Ebinuma (1983)/Byrd	0.464 ± 0.006	1.316 ± 0.006	41 ± 1
Ebinuma (1983)/Mizuho	0.423 ± 0.008	1.357 ± 0.006	37 ± 1
RICE (2004)/South Pole	0.43 ± 0.02	1.35 ± 0.02	71 ± 5
SPICE (2015)/South Pole	0.427 ± 0.004	1.353 ± 0.004	71 ± 2

Table 1: Fit parameters to measured $n(z)$ profiles. The function fit to the data is $n(z) = n_{ice} - \Delta n \exp(z/z_0)$. The differential equation derived in the first section requires $n_{ice} = 1.78$ and $\Delta n = n_{ice} - n(0)$ as boundary conditions.

PROPAGATION IN ANTARCTIC ICE

Fermat's Principle states that the observed ray follows the path that minimizes the optical path length, in the same sense as the principle of least action for a massive particle³. For an index that depends only on z , it can be expressed in Cartesian coordinates as:

$$\delta \int_A^B n(z)(1 + \dot{y}^2)^{1/2} dz = \delta \int_A^B L(z, \dot{y}) dz = 0 \quad (22)$$

Letting $u = dy/dz$, Eq. 23 follows from the Euler-Lagrange equations.

$$\dot{u} = - \left(\frac{\dot{n}}{n} \right) (u^3 + u). \quad (23)$$

³The z -coordinate is treated like time in these calculations.

PROPAGATION IN ANTARCTIC ICE

$$\dot{u} = - \left(\frac{\dot{n}}{n} \right) (u^3 + u). \quad (24)$$

We insert Eq. 21, and find two approximate cases:

1. Deep ice, $z \rightarrow -\infty$
2. Shallow ice, $\exp(z/z_0) \approx 1 + z/z_0$, and $u^3 \gg u$ (shallow ray)

Deep ice:

$$\dot{u} = 0 \quad (25)$$

Deep ice: the solution to this equation of motion is

$$z(y) = a + by \quad (26)$$

PROPAGATION IN ANTARCTIC ICE

$$\dot{u} = - \left(\frac{\dot{n}}{n} \right) (u^3 + u). \quad (27)$$

We insert Eq. 21, and find two approximate cases:

1. Deep ice, $z \rightarrow -\infty$
2. Shallow ice, $\exp(z/z_0) \approx 1 + z/z_0$, and $u^3 \gg u$ (shallow ray)

Shallow ice, shallow ray: the solution is quadratic, like

$$z(y) = -\frac{A}{Z_0} (y - y_0)^2 + B \quad (28)$$

Notice that the downward bending should be stronger for smaller z_0 values.

PROPAGATION IN ANTARCTIC ICE

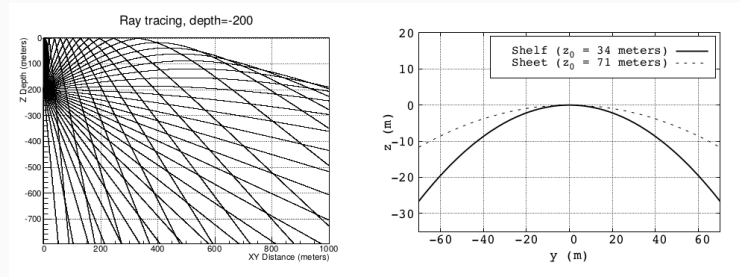


Figure 23: The two limiting solutions are apparent in our ray-tracing algorithms. The inability of RF waves to propagate horizontally in the firn is called *shadowing*.

PROPAGATION IN ANTARCTIC ICE

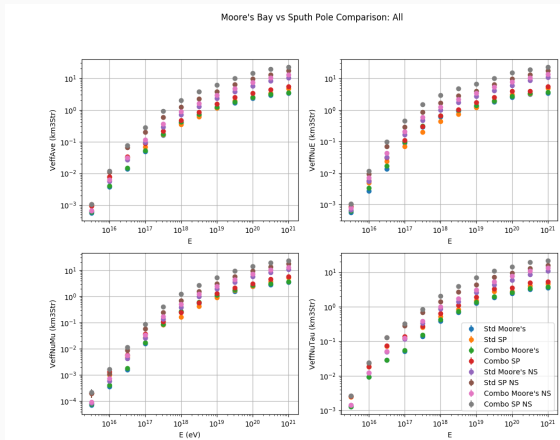


Figure 24: Comparison of different detector configurations in Monte Carlo simulation, toggling shadowing effect.

PROPAGATION IN ANTARCTIC ICE

- Classical propagation limits effective volume of the detectors by a factor of 2-10, depending on configuration.
- We should be able to measure more precisely this limitation with artificial RF pulses with initial horizontal velocities.

Over the past decade, many separate tests have been conducted...

1. Radio Ice Cherenkov Experiment (RICE) 2003-4, 2011
2. ARIANNA, Moore's Bay, 2011-12. PhD dissertation, J.C. Hanson (2013).
3. ARIANNA, Moore's Bay, 2016-17
4. ARA (2017-18) (see arXiv:1217.03301)

PROPAGATION IN ANTARCTIC ICE

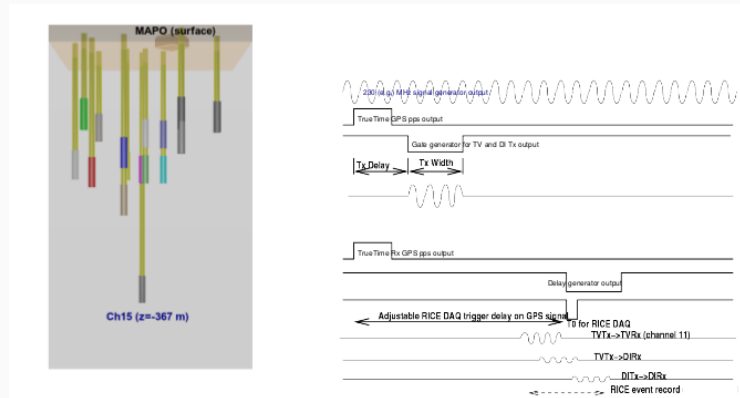


Figure 25: In the 2003-04 season, 230 MHz tone bursts were sent over 3km horizontally to the Radio Ice Cherenkov Experiment (RICE). The transmitter was at -70 m, -120 m, and -125 m. The receiver depths varied from 100-400 m.

PROPAGATION IN ANTARCTIC ICE

1. Expectation: shadowing should bend the signal away from receivers (No DI to DI, but yes TV to DI and TV to TV).
2. If signal is observed, should obey the following equation:

$$\frac{A_{far}}{A_{near}} = \frac{\cos \theta_{near}}{\cos \theta_{far}} \frac{r_{near}}{r_{far}} \times e^{-(r_{far} - r_{near})/L_{atten}} \quad (29)$$

- cosine terms account for gain of dipole transmitters, receivers
- L_{atten} is the *attenuation length*

PROPAGATION IN ANTARCTIC ICE

DI to DI signals observed.

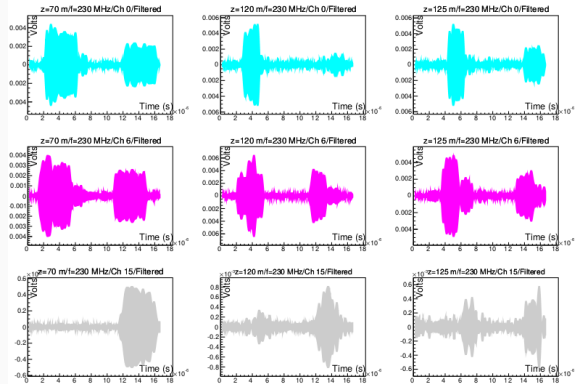


Figure 26: Varying receiver depth (left to right: -70 m, -120 m, and -125 m) and transmitter depth (top to bottom: -166 m, -170 m, and -367 m). (band-pass filter around 230 MHz).

PROPAGATION IN ANTARCTIC ICE

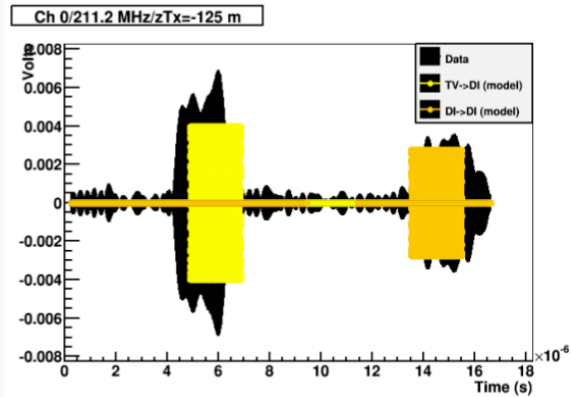


Figure 27: “Extreme” modeling of ray-path establishes close prediction of arrival times of TV and DI signals. Offsets are correspond to 0.02-0.03 systematic error in index of refraction (5%).

PROPAGATION IN ANTARCTIC ICE

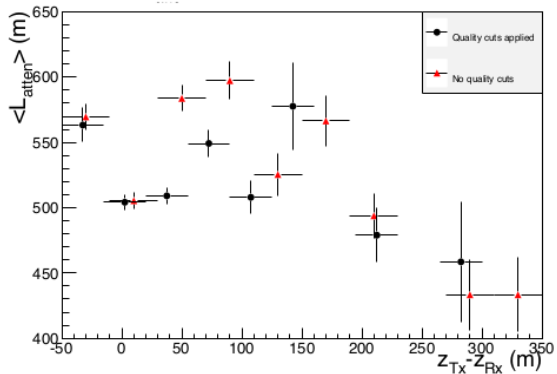


Figure 28: Extracting attenuation lengths from the data using Eq. 29 reveals $\bar{L}_{\text{atten}} = 550 \pm 10$ m. Either the systematic errors are 50 m, or this is an observation of z-dependent effects. Attenuation lengths are comparable to vertical measurements.

PROPAGATION IN ANTARCTIC ICE

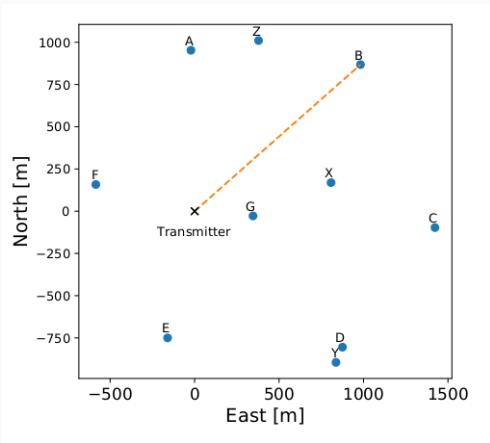


Figure 29: The ARIANNA HRA in 2016-17 season, with a DI transmitter at the origin. An example ray path is shown. Same expectations as the original RICE experiment - no signal due to shadowing.

PROPAGATION IN ANTARCTIC ICE

DI to DI signals observed, and DI to LPDA signals observed.

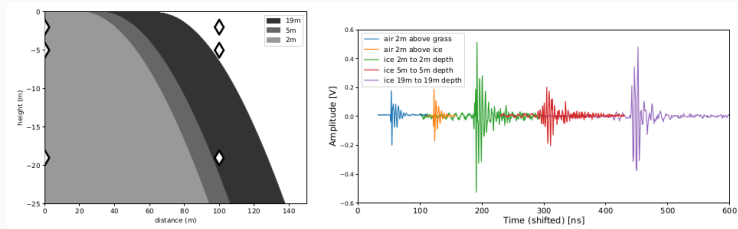


Figure 30: Two boreholes 100 meters apart and -19 m deep, DI to DI. DI signals also observed at far stations.

PROPAGATION IN ANTARCTIC ICE

DI to DI signals observed, and DI to LPDA signals observed.

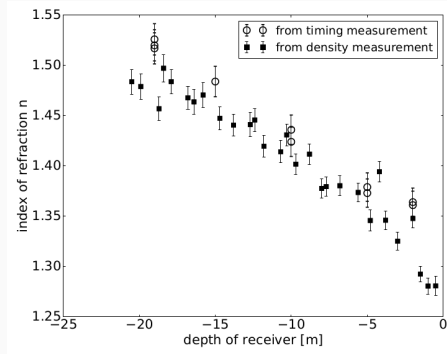


Figure 31: We have used data from the two boreholes (DI to DI) to extract $n(z)$ from propagation time, and compared to density measurements. There is a 1.5% systematic offset, compatible with $n_{air} = 1.016$ measured in air in California.

PROPAGATION IN ANTARCTIC ICE

DI to DI signals observed, and DI to LPDA signals observed.

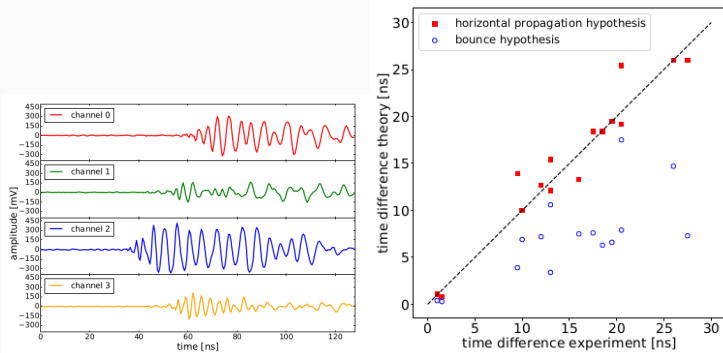


Figure 32: (Left) Signals observed 950 m from DI transmitter. Co-polarized signals are stronger. (Right) Arrival directions give LPDA-LPDA timing offsets consistent with horizontal propagation.

PROPAGATION IN ANTARCTIC ICE

DI to DI signals observed, and DI to LPDA signals observed.

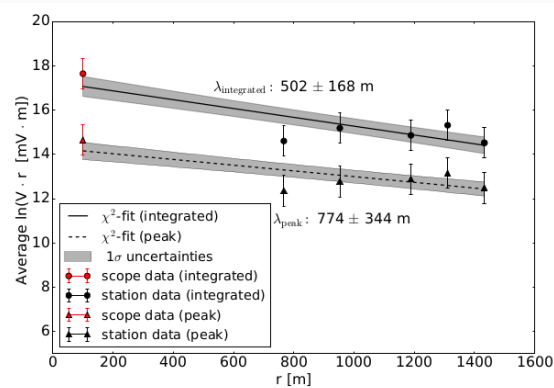


Figure 33: With many different channels on different stations observing the horizontal signals, L_{atten} is extracted. Two sets of points are derived from the signal waveforms, to probe dispersive effects.

PROPAGATION IN ANTARCTIC ICE

DI to DI signals observed, and DI to LPDA signals observed.

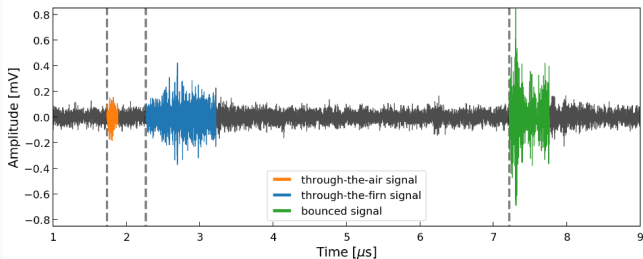


Figure 34: An LPDA connected to a scope and delay generator (which gives time reference), from DI transmitter at -19 m. The horizontal distance was 500 m. (Orange) in-air pulse, which disappears when RF pulser is disconnected from transmitter. (Blue) horizontal propagation, $n \approx 1.36$. (Green) Reflected signal, with known attenuation length and depth measurements from prior seasons [7].

PROPAGATION IN ANTARCTIC ICE

What is happening? Note: this is not strictly non-classical.

For example, consider a local perturbation:

$$n(z) = n_0 + a \exp\left(-\frac{1}{2} \frac{(z - z_d)^2}{2\sigma^2}\right) \quad (30)$$

$$\omega^2 = 2 \left(\frac{a}{n_0} \right) \quad (31)$$

$$q = (z - z_d)^2 \quad (32)$$

$$(\omega q / \sigma)^4 \ll 1 \quad (33)$$

$$z(y) = C_0 \sin\left(\pm C_1 \frac{\omega y}{\sigma} - C_2\right) \quad (34)$$

For the opposite sign of a in perturbation, we obtain hyperbolic rather than sinusoidal solutions. Notice that these perturbations do occur in the data, for both the South Pole and Moore's Bay.

PROPAGATION IN ANTARCTIC ICE

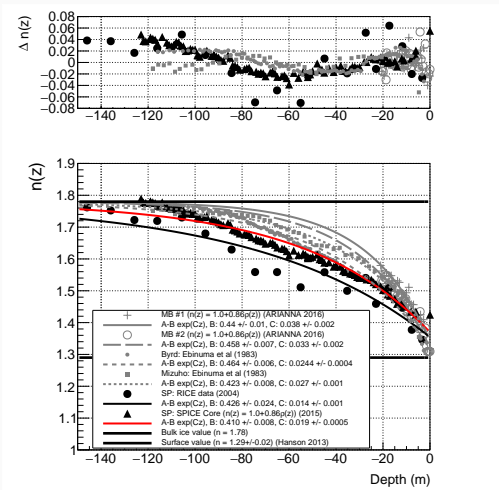


Figure 35: The density profile leads depth-dependence in $n(z)$.

CLASSICAL FORM OF THE PATH

CLASSICAL FORM OF THE PATH

We began with

$$\dot{u} = -\frac{\dot{n}}{n} (u^3 + u) \quad (35)$$

Let $v = -\ln n$. This allows

$$\frac{du}{dv} = u^3 + u \quad (36)$$

$$\ln u - \frac{1}{2} \ln(u^2 + 1) = v + C_0 \frac{dz}{dy} = \pm (C_0^2 n^2 - 1)^{1/2} \quad (37)$$

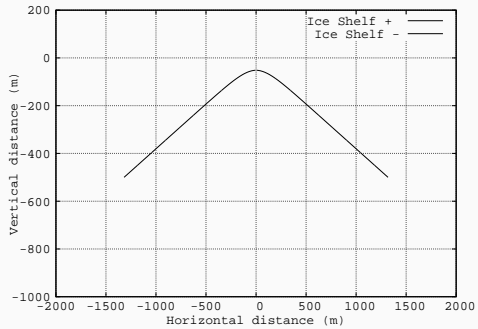
Let $\gamma = \Delta n \exp(z/z_0)$ so that $n(z) = n_{ice} - \gamma$. The final solution is...

CLASSICAL FORM OF THE PATH

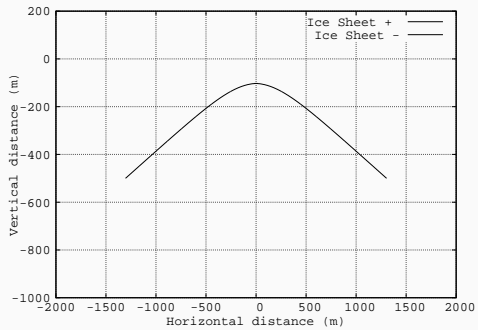
$$y(z) = \pm C_0^{-1} c^{-1/2} z_0 \ln \left\{ \frac{\gamma}{2c^{1/2}(\gamma^2 - b\gamma + c)^{1/2}} \right\} - z_0 C_1 \quad (38)$$

Where $b = 2n_{ice}$ and $c = n_{ice}^2 - C_0^{-2}$. The parameter C_0 controls the launch (viewing) angle, and C_1 is the initial horizontal displacement.

CLASSICAL FORM OF THE PATH



CLASSICAL FORM OF THE PATH



CONCLUSION

OUTLINE

- I. Cosmic rays ... *Ultra-high energy particles from space*
- II. Askaryan radiation ... *Classical and quantum physics*
- III. Antarctica... *Field of Askaryan-based cosmic ray science*
- IV. Propagation in Antarctic ice ... *New results*
 - 1. *Given the power in horizontal propagating RF waves in ice, we must re-evaluate detector design sensitivity*
 - 2. *This could lead to a hybrid detector, combining the best features of ARA and ARIANNA*
 - 3. *Horizontal attenuation lengths are comparable to vertical attenuation lengths*

REFERENCES

- [1] R. U. Abbasi and others. First Observation of the Greisen-Zatsepin-Kuzmin Suppression. *Phys. Rev. Lett.*, 100:101101, Mar 2008.
- [2] Patrick Allison, Jan Auffenberg, Robert Bard, JJ Beatty, DZ Besson, S Böser, C Chen, Pisin Chen, Amy Connolly, and Jonathan Davies. Design and initial performance of the askaryan radio array prototype eev neutrino detector at the south pole. *Astroparticle Physics*, 35(7):457–477, 12 2012.
- [3] Allison, P. and others. Performance of two askaryan radio array stations and first results in the search for ultrahigh energy neutrinos. *Phys. Rev. D*, 93:082003, Apr 2016.
- [4] S.W. Barwick, E.C. Berg, D.Z. Besson, G Binder, W.R. Binns, D.J. Boersma, R.G. Bose, D.L. Braun, J.H. Buckley, V Bugaev, S Buitink, K Dookayka, P.F. Dowkontt, T Duffin, S Euler, L Gerhardt, L Gustafsson, A Hallgren, J.C. Hanson, M.H. Israel, J Kiryluk, S.R. Klein, S Kleinfelder, H Niederhausen, M.A. Olevitch, C Persichelli, K Ratzlaff, B.F. Rauch, C Reed, M Roumi, A Samanta, G.E. Simburger, T Stezelberger, J Tatar, U.I. Uggerhoj, J Walker, G Yodh, and R Young. A first search for cosmogenic neutrinos with the arianna hexagonal radio array. *Astroparticle Physics*, 70:12–26, 2015.
- [5] SW Barwick, DZ Besson, A Burgman, E Chiem, A Hallgren, JC Hanson, SR Klein, S Kleinfelder, A Nelles, C Persichilli, S Phillips, T Prakash, C Reed, SR Shively, J Tatar, E Unger, J Walker, and G Yodh. Radio detection of air showers with the arianna experiment on the ross ice shelf. *Astroparticle Physics*, 2016.
- [6] PW Gorham, SW Barwick, JJ Beatty, DZ Besson, WR Binns, C Chen, P Chen, JM Clem, A Connolly, and PF Dowkontt. Observations of the askaryan effect in ice. *Physical review letters*, 99(17):171101, 7 2007.
- [7] Jordan C Hanson, Steven W Barwick, Eric C Berg, Dave Z Besson, Thorin J Duffin, Spencer R Klein, Stuart A Kleinfelder, Corey Reed, Mahshid Roumi, Thorsten Stezelberger, Joulien Tatar, James A Walker, and Liang Zou. Radar absorption, basal reflection, thickness and polarization measurements from the ross ice shelf, antarctica. *Journal of Glaciology*, 61(227):438–446, 2015.
- [8] Jordan C. Hanson and Amy L. Connolly. Complex analysis of askaryan radiation: A fully analytic treatment including the lpm effect and cascade form factor. *Astroparticle Physics*, 91:75–89, 2017.
- [9] J.J. Beatty, J. Matthews, S.P. Wakely. Particle Data Book, ch. 28. *Particle Data Group*, page 15, 2016.
- [10] J.J. Beatty, J. Matthews, S.P. Wakely. Particle Data Book, ch. 28. *Particle Data Group*, page 16, 2016.

- [11] P Miočinović, RC Field, PW Gorham, E Guillian, R Milinčić, D Saltzberg, D Walz, and D Williams. Time-domain measurement of broadband coherent cherenkov radiation. *Physical Review D*, 74(4):043002, 6 2006.
- [12] D Saltzberg, P Gorham, D Walz, C Field, R Iverson, A Odian, G Resch, P Schoessow, and D Williams. Observation of the askaryan effect: coherent microwave cherenkov emission from charge asymmetry in high-energy particle cascades. *Physical review letters*, 86(13):2802–5, 1 2001.